

## Probing the quantum noise of the spinon Fermi surface with NV centers

Jun Yong Khoo<sup>1,2</sup>, Falko Pientka<sup>3,2</sup>, Patrick A. Lee<sup>4</sup>, and Inti Sodemann Villadiego<sup>5,2</sup>


<sup>1</sup>*Institute of High Performance Computing, Agency for Science, Technology, and Research, Singapore 138632, Singapore*

<sup>2</sup>*Max-Planck-Institut für Physik komplexer Systeme, Nöthnitzer Strasse 38, 01187 Dresden, Germany*

<sup>3</sup>*Institut für Theoretische Physik, Goethe-Universität, 60438 Frankfurt am Main, Germany*

<sup>4</sup>*Department of Physics, Massachusetts Institute of Technology, Cambridge, Massachusetts 02139, USA*

<sup>5</sup>*Institut für Theoretische Physik, Universität Leipzig, Brüderstrasse 16, 04103 Leipzig, Germany*

 (Received 1 June 2022; revised 11 August 2022; accepted 12 August 2022; published 7 September 2022)

We study the transverse electrical conductivity and the corresponding magnetic noise of a two-dimensional U(1) spin liquid state with a spinon Fermi surface. We show that in the quasistatic regime these responses have the same wave-vector dependence as that of a metal but are reduced by a dimensionless prefactor controlled by the ratio of orbital diamagnetic susceptibilities of the spinons and chargons, correcting previous work. We estimate that this quasistatic regime is comfortably accessed by the typical nitrogen vacancy (NV) center splittings of a few gigahertz and estimate that the expected  $T_1$  times for an NV center placed above candidate materials, such as organic dmit and ET salts and monolayer  $1T$ -TaS<sub>2</sub>/Se<sub>2</sub>, would range from several tens to a few hundred milliseconds.

DOI: [10.1103/PhysRevB.106.115108](https://doi.org/10.1103/PhysRevB.106.115108)

### I. INTRODUCTION

Nitrogen vacancy (NV) centers are defects in diamond that carry a well-isolated spin [1] and have been finding promising applications in quantum computation [2–5], in quantum simulation [6,7], and also as powerful sensors of magnetic fields and magnetic noise correlations [8–10]. Their ability to measure local magnetic fields and their noise has recently attracted attention as a new technique to probe correlations and nonequilibrium states of metals [11–13] and could offer new ways to detect the elusive and complex quantum spin liquid states in correlated materials [14,15].

In its simplest mode of operation the magnetic noise is probed by measuring the spin relaxation time  $T_1$  of the NV center, which is inversely proportional to the autocorrelation function quantifying the temporal fluctuations of the magnetic field at the NV center location [1,8–10]. While the physics is conceptually similar to that controlling the  $T_1$  time of, e.g., nuclear spins embedded in the sample (as used in NMR techniques), the control of the NV center splitting as well as the control of its distance from the sample can allow for enhanced information on the frequency and wave-vector dependence of such magnetic fluctuations, which ultimately can provide enhanced information about the correlations in the sample that act as a source of such magnetic noise.

A recent work [15] showed that even when a metallic Fermi surface has a complex shape, the dissipative real part of the transverse conductivity is a universal quantity controlled entirely by its geometric shape, which in turn gives rise to a universal  $T_1$  time for an NV center controlled only by the length of the perimeter of the Fermi surface, in the regime where the NV center distance  $z$  satisfies  $p_F^{-1} \ll z \ll l_{\text{mfp}}$ , where  $p_F$  is the Fermi radius and  $l_{\text{mfp}}$  is the electron mean free path of the metal. However, while the conclusions of Ref. [15] on metallic Fermi surface states remain valid, the same work concluded incorrectly that the spinon Fermi surface state would have the same value for the low-frequency limit of the transverse conductivity and the associated  $T_1$  time as a metallic Fermi liquid.

The reason for this discrepancy is that Ref. [15] inadvertently missed the diamagnetic contributions of the spinons. As we will discuss here, the spinon transverse conductivity assumes a standard form of a Fermi liquid given by (in the limit  $\omega \ll v_F q \ll \epsilon_F$ ) [16,17]

$$\sigma_{\perp}^{\text{spinon}}(q, \omega) \approx \frac{e^2 p_F}{h q} + \chi_s \frac{q^2}{i\omega}. \quad (1)$$

Moreover, we will show that the expression for the physical transverse *electrical* conductivity of the spinon Fermi surface state (in the low-frequency limit) is given by

$$\sigma_{\perp}(q, \omega) \approx \left( \frac{\chi_c}{\chi_s + \chi_a + \chi_c} \right)^2 \frac{e^2 p_F}{h q} + \chi \frac{q^2}{i\omega}. \quad (2)$$

The above expressions apply in the zero-temperature and clean limit of a spin-degenerate, circular Fermi surface with radius  $p_F$ .  $\chi_{s,c}$  are spinon and chargon orbital diamagnetic susceptibilities,  $\chi_a$  is a diamagnetic susceptibility associated with the Maxwell term of the emergent U(1) gauge field,

Published by the American Physical Society under the terms of the [Creative Commons Attribution 4.0 International](https://creativecommons.org/licenses/by/4.0/) license. Further distribution of this work must maintain attribution to the author(s) and the published article's title, journal citation, and DOI. Open access publication funded by the Max Planck Society.

TABLE I. Order-of-magnitude estimates for material candidates (dmit stands for  $\text{EtMe}_3\text{Sb}[\text{Pd}(\text{dmit})_2]_2$  and  $\kappa$ -ET stands for  $\kappa$ -( $\text{ET})_2\text{Cu}_2(\text{CN})_3$ ). We took  $c = 0.5v_F$ ,  $F_1 = 0$ , and  $\chi_c = \chi_s + \chi_a$ , and for simplicity  $\epsilon_s = \epsilon_a = 0$ , so that the Mott scale  $\tilde{\omega}$  is determined by the chargon dielectric constant  $\epsilon_c$ . We have taken the temperature to be  $T = 10$  K, the NV center-to-sample distance to be  $z = 1$  nm, and the NV center splitting to be  $\omega = 3$  GHz (we take  $q = 1/z$  to estimate  $\Delta\omega_s$ ).  $\epsilon_F$  and  $\Delta\omega_s$  of  $1T$ - $\text{TaS}_2$  are left blank because they are still uncertain (see the discussion in the text). These values correct those of Table 2 in Ref. [15]. Notice that the above values are estimates for a single layer of each material. For multilayered or bulk samples we can add up the contributions of each layer, and there will be reduction of the  $T_1$  time by a factor of the order of  $T_1 \rightarrow T_1 \frac{d}{z \ln(l_{\text{mfp}}/z)} \sim T_1 \frac{d}{z}$ , where  $d$  is the interlayer distance (assuming  $l_{\text{mfp}} \gg z \gg d$ ).

	$k_F^{-1}$ (Å)	$\epsilon_F$ (meV)	$\omega_p$ (meV)	$\Delta\omega_s/2\pi$ (GHz)	$T_1$ (ms)
dmit	2.4	59	80 [27]	215	58
$\kappa$ -ET	3.2	98	87 [27]	$2 \times 10^3$	78
$1T$ - $\text{TaS}_2/\text{Se}_2$	4.4		200 [27]		109
$\text{WTe}_2$	26	29	60 [18]	$6 \times 10^4$	630

and  $\chi^{-1} = (\chi_s + \chi_a)^{-1} + \chi_c^{-1}$ . Therefore, we see that while the transverse conductivity has the same form as that of an ordinary metal in this quasistatic regime, its real (dissipative) part is corrected by the dimensionless factor  $\chi_c^2/(\chi_s + \chi_a + \chi_c)^2$ . As a consequence, the remarkable result of Ref. [15] that the relaxation rate  $1/T_1$  of an NV center coupled to a two-dimensional spinon Fermi surface state has the same dependence on distance, frequency, and temperature as in the metallic case remains valid, albeit with an extra prefactor,  $\chi_c^2/(\chi_s + \chi_a + \chi_c)^2$  (see Table I for specific estimates).

## II. SPINON FERMI SURFACE LOW-ENERGY THEORY

The following low-energy effective Lagrangian captures the orbital coupling of the spinon Fermi surface state to the physical electromagnetic fields (denoted by  $\mathbf{E} = -\partial_r\phi - \partial_t\mathbf{A}$  and  $\mathbf{B} = \partial_r \times \mathbf{A}$ ):

$$\mathcal{L} = \mathcal{L}_{\text{spinon}}(\mathbf{p} - \mathbf{a}) + \mathcal{L}_{\text{chargon}}(\mathbf{p} - \mathbf{A} + \mathbf{a}) + \frac{\epsilon_a}{2}\mathbf{e}^2 - \frac{\chi_a}{2}\mathbf{b}^2 + \dots \quad (3)$$

Let us briefly explain the physical meaning of the various terms. Here we are imagining that deconfinement of the  $U(1)$  gauge field has taken place and thus the emergent electric and magnetic fields, denoted by  $\mathbf{e} = -\partial_r\phi - \partial_t\mathbf{a}$  and  $\mathbf{b} = \partial_r \times \mathbf{a}$ , can be taken to be noncompact. The emergent gauge field now acquires dynamics which is described by a Maxwell-like term and parametrized by emergent dielectric and diamagnetic constants  $\epsilon_a$  and  $\chi_a$ .  $\mathcal{L}_{\text{spinon}}(\mathbf{p} - \mathbf{a})$  is shorthand for the Lagrangian of a fermion (the spinon) minimally coupled to the emergent  $U(1)$  gauge field  $\mathbf{a}$  but neutral under the physical gauge field  $\mathbf{A}$ . On the other hand,  $\mathcal{L}_{\text{chargon}}(\mathbf{p} - \mathbf{A} + \mathbf{a})$  describes the Lagrangian of a boson (the chargon) that minimally couples to the physical field and carries a gauge charge opposite that of the spinon with respect to the emergent field. The above Lagrangian can be motivated from a slave-boson (or the closely related slave-rotor [19]) parton decomposition

of the electron operator, which is viewed as the composite of the spinon and chargon (see, e.g., [20,21]). Nevertheless, we would like to emphasize that in the above Lagrangian the spinon and chargon should not be viewed, strictly speaking, as the same objects as the unphysical UV partons, but rather as low-energy deconfined physical quasiparticles. In fact, due to the presence of the Maxwell term, if we were to change the Lagrangian in Eq. (3) by coupling the spinon to the physical gauge field instead of the chargon, we would obtain different predictions for physical gauge-invariant observables. Therefore, in this sense, we no longer have the freedom to assign the coupling of the electromagnetic field to either the chargon or the spinon and get the same answer.

Because the chargons are gapped, they can be integrated out for the purpose of the low-energy description, and thus, their Lagrangian can be replaced by a Maxwell term of the form

$$\mathcal{L}_{\text{chargon}}(\mathbf{p} - \mathbf{A} + \mathbf{a}) \approx \frac{\epsilon_c}{2}(\mathbf{e} - \mathbf{E})^2 - \frac{\chi_c}{2}(\mathbf{b} - \mathbf{B})^2. \quad (4)$$

The effective dielectric and diamagnetic constants of the chargons,  $\epsilon_c$  and  $\chi_c$ , will depend on their detailed microscopic dispersion. For example, within a relativistic boson model of the chargon dispersion, one obtains  $\chi_c = 1/(24\pi m_c)$ , where  $m_c = \Delta_c/v_c^2$  is the effective mass of the chargons with a speed  $v_c$  and a gap  $\Delta_c$ , as shown in Ref. [22].

On the other hand, for the spinons, one can keep track of their occupation of momentum states only within a narrow sliver around the Fermi surface while integrating out higher-energy modes. This amounts to replacing  $\mathcal{L}_{\text{spinon}}$  by the following Lagrangian:

$$\mathcal{L}_{\text{spinon}}(\mathbf{p} - \mathbf{a}) \approx \mathcal{L}_{\text{spinon}}^{FS}(\mathbf{p} - \mathbf{a}) + \frac{\epsilon_s}{2}\mathbf{e}^2 - \frac{\chi_s}{2}\mathbf{b}^2. \quad (5)$$

The Maxwell terms for the emergent electromagnetic fields arise from integrating out the modes away from the Fermi surface; in particular, the magnetic term accounts for the spinon diamagnetism  $\chi_s$ . These terms were missed in Ref. [15]. For a nonrelativistic parabolic dispersion for the spinons one obtains  $\chi_s = g_s/(24\pi m_s)$  (namely, the standard Landau diamagnetic constant with  $g_s = 2$  accounting for the spin degeneracy).

Next, we follow the classic work of Ioffe and Larkin [23] to derive a relation between the physical conductivity and the spinon and chargon conductivities. Due to the appearance of the Maxwell term in Eq. (3), which was absent in the original Ioffe-Larkin paper, the derivation is a little different, and the result is slightly modified. First, the Euler-Lagrange equation of motion that follows from Eq. (3), by taking its variational derivatives with respect to  $\mathbf{a}$ ,  $\delta\mathcal{L}/\delta\mathbf{a} = 0$ , is given by

$$\chi_a\partial_r \times \mathbf{b} - \epsilon_a\partial_t\mathbf{e} = \mathbf{j}_s - \mathbf{j}_c, \quad (6)$$

where  $\mathbf{j}_s = \delta\mathcal{L}_{\text{spinon}}/\delta\mathbf{a}$  and  $\mathbf{j}_c = -\delta\mathcal{L}_{\text{chargon}}/\delta\mathbf{a}$  are the spinon and chargon current densities, respectively. Second, by taking functional derivatives with respect to the physical gauge field, we find that

$$\mathbf{j}_e = \frac{\delta\mathcal{L}}{\delta\mathbf{A}} = \mathbf{j}_c, \quad (7)$$

so that the physical electric current density  $\mathbf{j}_e$  is the same as the chargin current  $\mathbf{j}_c$  but is modified from the spinon current. To obtain explicit dependence on the electric fields, we use Faraday's law  $\partial_r \times \mathbf{e} = -\partial_t \mathbf{b}$  to eliminate  $\mathbf{b}$  in Eq. (6). It is convenient to decompose the currents into perpendicular and transverse components and define the corresponding conductivity as

$$\begin{aligned} \mathbf{j}_{e\perp} &= \sigma_{\perp} \mathbf{E}_{\perp}, \\ \mathbf{j}_{s\perp} &= \sigma_{s\perp} \mathbf{e}_{\perp}, \\ \mathbf{j}_{c\perp} &= \sigma_{c\perp} (\mathbf{E}_{\perp} - \mathbf{e}_{\perp}), \end{aligned} \quad (8)$$

with similar notation for the longitudinal components. Going to Fourier space, we find the relations between  $\mathbf{e}$  and  $\mathbf{E}$ :

$$\begin{aligned} (\sigma_{c\parallel} + \sigma_{s\parallel} + i\epsilon_a \omega) \mathbf{e}_{\parallel} &= \sigma_{c\parallel} \mathbf{E}_{\parallel}, \\ \left( \sigma_{c\perp} + \sigma_{s\perp} + i\epsilon_a \omega + \chi_a \frac{q^2}{i\omega} \right) \mathbf{e}_{\perp} &= \sigma_{c\perp} \mathbf{E}_{\perp}, \end{aligned} \quad (9)$$

where the conductivities are understood to be frequency and wave vector dependent. It is convenient to introduce

$$\begin{aligned} \sigma'_{s\parallel} &\equiv \sigma_{s\parallel} + i\epsilon_a \omega, \\ \sigma'_{s\perp} &\equiv \sigma_{s\perp} + i\epsilon_a \omega + \chi_a \frac{q^2}{i\omega}. \end{aligned} \quad (10)$$

Then, by using Eqs. (7) and (8) to compute  $\sigma$  and using Eq. (9) to eliminate  $\mathbf{e}$ , we arrive at a result with the same form as the classic Ioffe-Larkin formula,  $\sigma^{-1} = \sigma_c^{-1} + \sigma_s'^{-1}$ . The longitudinal and transverse components of the physical conductivity  $\sigma$  are

$$\sigma_{\parallel}^{-1}(q, \omega) = \sigma_{c\parallel}^{-1}(\omega) + [\sigma_{s\parallel}(q, \omega) + i\omega\epsilon_a]^{-1}, \quad (11)$$

$$\sigma_{\perp}^{-1}(q, \omega) = \sigma_{c\perp}^{-1}(q, \omega) + \left( \sigma_{s\perp}(q, \omega) + i\omega\epsilon_a + \chi_a \frac{q^2}{i\omega} \right)^{-1}. \quad (12)$$

Compared with the standard Ioffe-Larkin formula, the spinon conductivity has extra terms which are proportional to  $\epsilon_a$  and  $\chi_a$ .

Now we apply Eq. (12) to the problem at hand. Since we are interested in the limit  $\omega \ll v_F q \ll \epsilon_F$ , we can drop the term  $i\omega\epsilon_a$  in Eq. (12). We first treat the spinon as a free Fermi liquid and use the form given by Eq. (1) for  $\sigma_{s\perp}$ . Since the chargin is gapped, we set  $\sigma_{c\perp} = \chi_c \frac{q^2}{i\omega}$ . Making the above substitutions in Eq. (12), we obtain our main result given by Eq. (2). The first term is the real (dissipative) part that enters into the calculation of the relaxation rate of the NV center. As noted in the Introduction, it is reduced from that of a metal by the factor  $\chi_c^2 / (\chi_s + \chi_a + \chi_c)^2$ . We can interpret this result as originating from the fact that the physical fluctuating current is reduced from that of a free Fermi sea by the factor  $F = \chi_c / (\chi_s + \chi_a + \chi_c)$  because its flow is restricted by coupling to the emergent gauge field. The conductivity is suppressed by  $F^2$  because it is proportional to a product of two current operators. It is also worth noting that when compared with the standard Ioffe-Larkin formula,  $\chi_s$  is replaced by  $\chi_s + \chi_a$ . Thus, the appearance of the Maxwell term in the gauge field Lagrangian can be absorbed as a redefinition of the spinon

diamagnetic susceptibility if one chooses to use the original Ioffe-Larkin formula.

In Ref. [15] the spinon conductivity was treated more accurately, including Fermi liquid corrections due to the scattering of quasiparticles near the Fermi surface, as well as accounting for Landau parameters. For completeness, below, we give the relevant formulas which can be plugged into Eq. (12) to give the physical conductivity. Nevertheless, as we will see, in the low-frequency limit  $\omega \ll v_F q \ll \epsilon_F$  and clean limit  $q \gg l_{\text{mfp}}^{-1}$  (see the discussion in Sec. III), the same reduction factor  $F^2$  appears in the dissipative part of the conductivity which enters into the relaxation rate of the NV center, and therefore, we recover the same limit as in Eq. (2) even within this more accurate description of the spinon conductivity.

The contribution to the spinon density  $\rho_{\text{FS}}$  and current  $\mathbf{j}_{\text{FS}}$  arising from fluctuations in the vicinity of the Fermi surface can be expressed in terms of the change in the spinon occupation near the Fermi surface  $\delta n_p$  as follows:

$$\rho_{\text{FS}} = \frac{1}{\mathcal{A}} \sum_p \delta n_p, \quad \mathbf{j}_{\text{FS}} = \frac{1}{\mathcal{A}} \sum_p \mathbf{v}_p \delta \bar{n}_p, \quad (13)$$

$$\delta \bar{n}_p = \delta n_p + \sum_{p'} f_{pp'} \delta(\epsilon_p - \epsilon_{p'}) \delta n_{p'}, \quad (14)$$

where  $\mathbf{v}_p = \partial_p \epsilon(\mathbf{p})$  is the spinon quasiparticle velocity and  $f_{p,p'}$  accounts for Landau parameters. The spinon distribution function obeys the linearized kinetic equation

$$\partial_t \delta n_p + \mathbf{v}_p \cdot \partial_r \delta \bar{n}_p + \mathbf{e} \cdot \mathbf{v}_p \delta(\epsilon_p - \epsilon_F) = I[\delta n_p], \quad (15)$$

where  $I[\delta n_p]$  accounts for momentum-relaxing and momentum-preserving collisions with the respective scattering rates  $\Gamma_1$  and  $\Gamma_2$  based on the model for collisions described in Refs. [15,24–26]. By solving the kinetic equation for a circular Fermi surface, one obtains the following expressions for the different conductivities:

$$\sigma_{s\parallel} = i \frac{n}{m} \left[ \frac{2}{\frac{2in}{m} \rho_*(q, \omega) + F_1 \omega_- - \omega_+ - 2i\Gamma_2} \right] + i\omega\epsilon_s, \quad (16)$$

$$\sigma_{s\perp} = i \frac{n}{m} \left[ \frac{2}{F_1 \omega_- - \omega_+ - 2i\Gamma_2} \right] + i\omega\epsilon_s + \chi_s \frac{q^2}{i\omega}, \quad (17)$$

$$\rho_*(q, \omega) = -i \frac{1}{n^2 \kappa} \frac{q^2}{\omega}, \quad \kappa = \frac{1}{n E_F} \frac{1}{1 + F_0}, \quad (18)$$

$$\omega_{\pm} = \omega - i(\Gamma_1 + \Gamma_2) \pm \sqrt{[\omega - i(\Gamma_1 + \Gamma_2)]^2 - (v_F q)^2}, \quad (19)$$

$$\sigma_{c\parallel} = i\omega\epsilon_c, \quad \sigma_{c\perp} = i\omega\epsilon_c + \chi_c \frac{q^2}{i\omega}, \quad (20)$$

where  $n = p_F^2 / 4\pi$  is the spinon density,  $E_F = p_F^2 / 2m^*$  is the Fermi energy, and we have included only two nonzero Landau parameters,  $F_0$  and  $F_1$ . The Landau parameter  $F_1$  determines the renormalization of the spinon quasiparticle mass  $m^*$  relative to its transport mass  $m$ :  $m = m^* / (1 + F_1)$ . The above expressions from Eqs. (20) can then be plugged onto Eq. (12).

Although we focus on the properties of the transverse conductivity in this study, we mention in passing that the optical

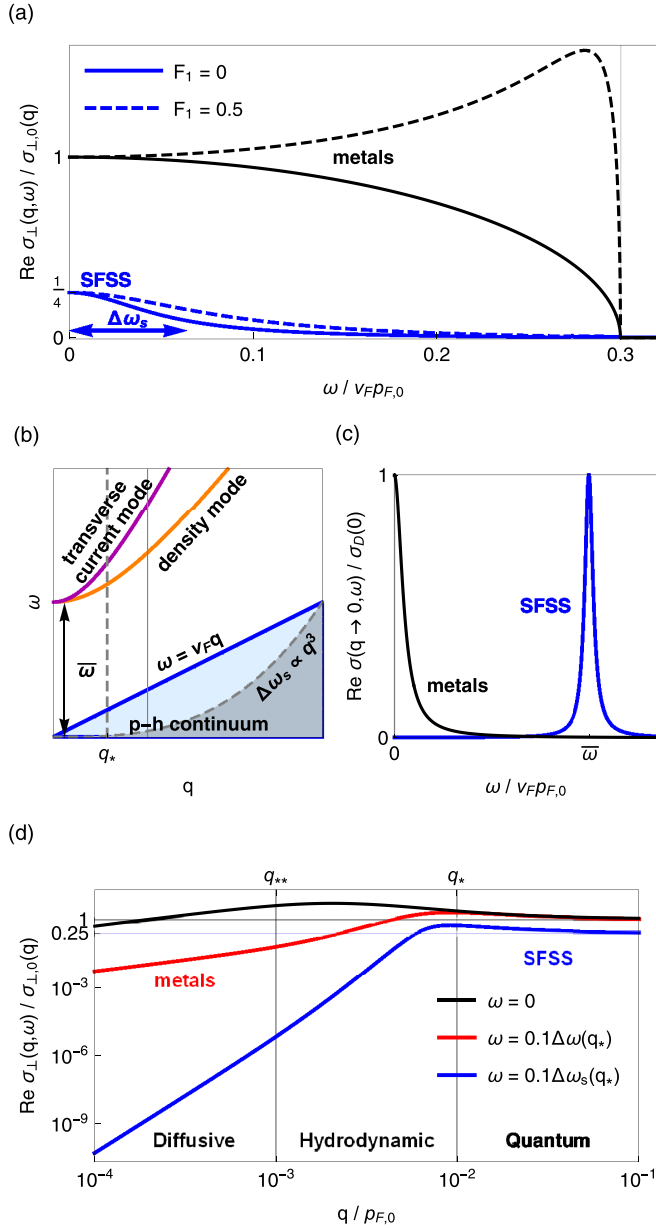


FIG. 1. Comparison of the conductivity of the spinon Fermi surface state (SFSS; blue) and a metal (black). This corrects Fig. 3 in Ref. [15] by including the spinon Landau diamagnetism. (a)  $\text{Re} \sigma_{\perp}(q, \omega)$  for  $q = 0.3 p_{F,0}$  [along the solid vertical line cut in (b)]. (b) Dispersion of collective modes and particle-hole excitations in the spinon Fermi surface state ( $F_I = 0$ ). (c)  $\text{Re} \sigma_{\parallel}(q \rightarrow 0, \omega)$  with weak collisions:  $\Gamma_1 = \Gamma_2 = 0.1 v_F p_{F,0}$ . In (b) and (c) the optical pseudogap is  $\bar{\omega}$  (see Supplemental Material [28] for details). (d)  $\text{Re} \sigma_{\perp}(q, \omega)$  at different (small) frequencies. We take here  $\chi_s + \chi_a = \chi_c$  and  $\epsilon_s = \epsilon_a = 0$ .

conductivity peaks at some typical scale that can be viewed as the optical pseudogap associated with the Mott scale (see Fig. 1 and further information in Ref. [28]). The expression for this scale is

$$\bar{\omega} = \sqrt{\frac{n}{m(\epsilon_c + \epsilon_s + \epsilon_a)}}. \quad (21)$$

### III. CONDUCTIVITIES AND MAGNETIC NOISE OF THE SPINON FERMI SURFACE STATE

As discussed in Ref. [15], the clean limit of the quasistatic conductivity is attained for wave vectors above an inverse spinon mean free path,  $q \gg l_{\text{mfp}}^{-1}$ , given by

$$l_{\text{mfp}}^{-1} = \max(q_C, q_D), \quad (22)$$

$$v_F q_D = \frac{2\Gamma_1}{(1 + F_1)}, \quad v_F q_C = (\Gamma_1 + \Gamma_2). \quad (23)$$

In this wave-vector regime, Eq. (2) can be obtained by taking the limit  $\omega \rightarrow 0$  from the expressions in Eqs. (11)–(20). At fixed wave vector but finite frequency, the real part of the transverse conductivity vanishes above a typical frequency window  $\Delta\omega_s$ , as illustrated in Fig. 1, which can be estimated to be

$$\frac{\Delta\omega_s}{2\pi} \simeq \frac{(\chi_c + \chi_s + \chi_a)q^3}{p_F}. \quad (24)$$

Hence, measuring the quasistatic conductivity requires experiments to operate at frequencies  $\omega \ll \Delta\omega_s$ . NV centers have a level splitting of about 3 GHz [10], well below typical values for  $\Delta\omega_s$  listed in Table I, making them ideally suited to probe the quasistatic regime of the conductivity. As we will see later on, the main challenge is their rather weak coupling to the spin liquid, which leads to relatively long  $T_1$  times.

In the more general case of a noncircular spinon Fermi surface, the real part of the quasistatic transverse conductivity (at low temperatures and for  $p_F^{-1} \gg q \gg 1/l_{\text{mfp}}$ ) is given by

$$\text{Re} \sigma_{\perp} = \left( \frac{\chi_c}{\chi_s + \chi_a + \chi_c} \right)^2 (2S + 1) \frac{e^2}{2\hbar q} \sum_i \mathcal{R}_{\text{F}}|_{p_i^*(\hat{q})}, \quad (25)$$

where  $(2S + 1)$  is the spin degeneracy factor,  $\{p_i^*\}$  is the set of points on the Fermi surface at which the Fermi velocity is orthogonal to  $\hat{q}$ , and  $\mathcal{R}_{\text{F}}|_{p_i^*(\hat{q})}$  is the absolute value of the local radius of curvature of the Fermi surface at  $p_i^*$ . Therefore, the conductivity depends only on the geometry of the Fermi surface and is reduced by the same factor,  $\chi_c^2/(\chi_s + \chi_a + \chi_c)^2$ , as in the case of metals described in Ref. [15].

The above quasistatic transverse conductivity can be probed by measuring the  $T_1$  time of a single spin (NV center) placed above the sample at distance  $z$  [10,14,29]. This  $T_1$  time is inversely proportional to the imaginary part of the magnetic field autocorrelation function (magnetic noise) at the NV center location,  $\text{Im} \chi_{B_{\mu} B_{\nu}}(z, \omega)$  and at the frequency  $\omega$  given by the energy splitting of the NV center [10,30]. For the circular Fermi surface, we have

$$\text{Im} \chi_{B_{\mu} B_{\nu}}(z, \omega) = \frac{\mu_0^2 \omega}{8\pi} \int q dq e^{-2qz} \text{Re} \sigma_{\perp}(q, \omega). \quad (26)$$

More general expressions are discussed in Ref. [15]. With our complete expressions for the conductivity from Eqs. (11)–(20), we plot the above autocorrelation function at low frequencies in Fig. 2 as a function of the NV center distance  $z$ . We see that when the distance of the NV center is smaller than the spinon mean free path ( $p_F^{-1} \ll z \ll l_{\text{mfp}}$ ), the magnetic noise approaches the following universal value at low

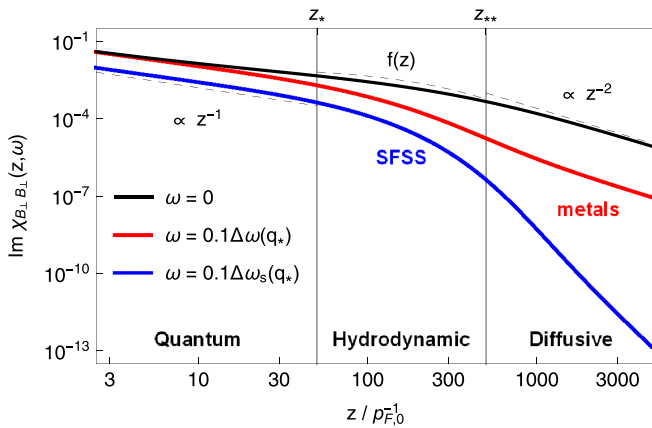


FIG. 2. Magnetic noise of the SFSS (blue) analogous to those shown in Fig. 5 in Ref. [15], but including the Landau diamagnetism, for  $\epsilon_s = \epsilon_a = 0$  and  $\chi_s = \chi_c$ . The analogous behavior of the metals is shown by the black and red curves.

frequencies:

$$\text{Im}\chi_{B_z B_z} \simeq \left( \frac{\chi_c}{\chi_s + \chi_a + \chi_c} \right)^2 \frac{e^2 \mu_0^2 \omega (2S + 1)}{16\pi \hbar z} \mathcal{P}_{\text{FS}}, \quad (27)$$

with subleading corrections to the above starting at  $O(\omega^3)$ . The above formula applies to Fermi surfaces of arbitrary shapes, and here  $\mathcal{P}_{\text{FS}}$  is the length of the perimeter of the spinon Fermi surface, which in the case of the circle is  $\mathcal{P}_{\text{FS}} = 2\pi p_F$ . The above expression contains the dimensionless prefactor,  $\chi_c^2 / (\chi_s + \chi_a + \chi_c)^2$ , which was missing in Ref. [15]. From the above we estimate the  $T_1$  times in Table I using the following formula [10,30]:

$$\frac{1}{T_1} = \frac{\mu_B^2}{2\hbar} \coth\left(\frac{\beta \hbar \omega}{2}\right) \text{Im}\chi_{B_z B_z}(z, \omega), \quad (28)$$

where here we have simply set the magnetic moment of the NV to be the Bohr magneton for purposes of order-of-magnitude estimates. For Table I we take  $z = 1$  nm,  $\omega = 3$  GHz, and  $T = 10$  K as parameters for the NV center [10]. The search for potential spin liquid states in 1T-TaS<sub>2</sub> and 1T-TaSe<sub>2</sub> [31–34] might be simpler in monolayers compared to bulk samples, as there are two possible types of surfaces for the latter: an unpaired single layer or a paired double layer [35]. Unfortunately, so far the specific heat has been measured only in bulk samples, which complicates the extraction of

the spinon Fermi energy from bulk measurements, such as the specific heat [36]. This is why we do not indicate values for  $\epsilon_F$  and  $\Delta\omega_s$  in Table I. Nevertheless, the estimate of the  $T_1$  time can be performed without detailed knowledge of the spinon Fermi energy scale, thanks to its simple dependence on the length of the perimeter of the Fermi surface (which can be estimated from the spinon density). This is why we have been able to provide an estimate of the expected  $T_1$  time of 1T-TaS<sub>2</sub>/Se<sub>2</sub> in Table I.

We also would like to mention in passing that the discussion in this work does not necessarily apply to the “pseudoscalar” spinon Fermi surface introduced in Ref. [37] to explain the oscillations of thermal conductivity in  $\alpha$ -RuCl<sub>3</sub> [38,39].

#### IV. SUMMARY AND OUTLOOK

We have shown that in the regime of wave vectors  $l_{\text{mfp}}^{-1} \ll q \ll p_F$ , the dissipative part of the transverse electrical conductivity of a spinon Fermi surface state has the same form as that of a metal, but it is multiplied by the overall prefactor  $\chi_c^2 / (\chi_s + \chi_a + \chi_c)^2$ , where  $\chi_{s/c}$  are the spinon and chargon orbital diamagnetic susceptibilities and  $\chi_a$  is the diamagnetic susceptibility of the emergent U(1) gauge field, correcting the results of Ref. [15]. Interestingly, this prefactor also controls the effective magnetic field that the spinons experience in response to a physical magnetic field and, consequently, the period of their quantum oscillations [40–42].

The  $1/T_1$  decay rate of an NV center placed near the spin liquid is therefore determined by the product of this prefactor and the length of the perimeter of the spinon Fermi surface, according to Eqs. (27) and (28). We have estimated  $T_1$  times for several spinon Fermi surface candidate materials and found that they range from a few tens of to a few hundred milliseconds, as summarized in Table I. The remaining challenge, therefore, is to attain the experimental conditions required to measure these relatively long  $T_1$  times. Nonetheless, NV centers are ideally suited for measuring the quasistatic regime of the transverse conductivity as they probe frequencies of the order of gigahertz, which are very small compared to the typical energy scales of these systems.

#### ACKNOWLEDGMENT

P.A.L. acknowledges the support from DOE Office of Basic Sciences Grant No. DE-FG02-03ER46076.

- [1] M. W. Doherty, N. B. Manson, P. Delaney, F. Jelezko, J. Wrachtrup, and L. C. Hollenberg, *Phys. Rep.* **528**, 1 (2013).
- [2] J. Wrachtrup, S. Y. Kilin, and A. Nizovtsev, *Opt. Spectrosc.* **91**, 429 (2001).
- [3] S. Praver and A. D. Greentree, *Science* **320**, 1601 (2008).
- [4] L. Childress and R. Hanson, *MRS Bull.* **38**, 134 (2013).
- [5] S. Pezzagna and J. Meijer, *Appl. Phys. Rev.* **8**, 011308 (2021).
- [6] J. Cai, A. Retzker, F. Jelezko, and M. B. Plenio, *Nat. Phys.* **9**, 168 (2013).
- [7] C. Ju, C. Lei, X. Xu, D. Culcer, Z. Zhang, and J. Du, *Phys. Rev. B* **89**, 045432 (2014).
- [8] R. Schirhagl, K. Chang, M. Loretz, and C. L. Degen, *Annu. Rev. Phys. Chem.* **65**, 83 (2014).
- [9] L. Rondin, J.-P. Tetienne, T. Hingant, J.-F. Roch, P. Maletinsky, and V. Jacques, *Rep. Prog. Phys.* **77**, 056503 (2014).
- [10] F. Casola, T. van der Sar, and A. Yacoby, *Nat. Rev. Mater.* **3**, 17088 (2018).
- [11] S. Kolkowitz, A. Safira, A. A. High, R. C. Devlin, S. Choi, Q. P. Unterreithmeier, D. Patterson, A. S. Zibrov, V. E. Manucharyan, H. Park, and M. D. Lukin, *Science* **347**, 1129 (2015).
- [12] A. Ariyaratne, D. Bluvstein, B. A. Myers, and A. C. B. Jayich, *Nat. Commun.* **9**, 2406 (2018).

- [13] J.-P. Tetienne, N. Dontschuk, D. A. Broadway, A. Stacey, D. A. Simpson, and L. C. Hollenberg, *Sci. Adv.* **3**, e1602429 (2017).
- [14] S. Chatterjee, J. F. Rodriguez-Nieva, and E. Demler, *Phys. Rev. B* **99**, 104425 (2019).
- [15] J. Khoo, F. Pientka, and I. Villadiego, *New J. Phys.* **23**, 113009 (2021).
- [16] D. Pines and P. Nozières, *Theory of Quantum Liquids: Normal Fermi Liquids* (CRC Press, Boca Raton, FL, 2018).
- [17] G. Giuliani and G. Vignale, *Quantum Theory of the Electron Liquid* (Cambridge University Press, Cambridge, 2005).
- [18] P. Wang, G. Yu, Y. Jia, M. Onyszczyk, F. A. Cevallos, S. Lei, S. Klemenz, K. Watanabe, T. Taniguchi, R. J. Cava, L. M. Schoop, and S. Wu, *Nature (London)* **589**, 225 (2021).
- [19] S. Florens and A. Georges, *Phys. Rev. B* **70**, 035114 (2004).
- [20] P. A. Lee, N. Nagaosa, and X.-G. Wen, *Rev. Mod. Phys.* **78**, 17 (2006).
- [21] T. Senthil, *Phys. Rev. B* **78**, 045109 (2008).
- [22] Z. Dai, T. Senthil, and P. A. Lee, *Phys. Rev. B* **101**, 064502 (2020).
- [23] L. B. Ioffe and A. I. Larkin, *Phys. Rev. B* **39**, 8988 (1989).
- [24] L. Levitov and G. Falkovich, *Nat. Phys.* **12**, 672 (2016).
- [25] H. Guo, E. Ilseven, G. Falkovich, and L. S. Levitov, *Proc. Natl. Acad. Sci. USA* **114**, 3068 (2017).
- [26] P. S. Alekseev and M. A. Semina, *Phys. Rev. B* **98**, 165412 (2018).
- [27] P. Rao and I. Sodemann, *Phys. Rev. B* **100**, 155150 (2019).
- [28] See Supplemental Material at <http://link.aps.org/supplemental/10.1103/PhysRevB.106.115108> for details of the spinon Fermi surface state quasi-static transverse conductivity, optical pseudo-gap, and the diamagnetic correction to Landau Fermi liquid theory.
- [29] K. Agarwal, R. Schmidt, B. Halperin, V. Oganesyan, G. Zaránd, M. D. Lukin, and E. Demler, *Phys. Rev. B* **95**, 155107 (2017).
- [30] L. S. Langsjoen, A. Poudel, M. G. Vavilov, and R. Joynt, *Phys. Rev. A* **86**, 010301(R) (2012).
- [31] K. T. Law and P. A. Lee, *Proc. Natl. Acad. Sci. USA* **114**, 6996 (2017).
- [32] W.-Y. He, X. Y. Xu, G. Chen, K. T. Law, and P. A. Lee, *Phys. Rev. Lett.* **121**, 046401 (2018).
- [33] W. Ruan *et al.*, *Nat. Phys.* **17**, 1154 (2021).
- [34] C. Chen, I. Sodemann, and P. A. Lee, *Phys. Rev. B* **103**, 085128 (2021).
- [35] C. Butler, M. Yoshida, T. Hanaguri, and Y. Iwasa, *Nat. Commun.* **11**, 1 (2020).
- [36] A. Ribak, I. Silber, C. Baines, K. Chashka, Z. Salman, Y. Dagan, and A. Kanigel, *Phys. Rev. B* **96**, 195131 (2017).
- [37] I. Sodemann Villadiego, *Phys. Rev. B* **104**, 195149 (2021).
- [38] P. Czajka, T. Gao, M. Hirschberger, P. Lampen-Kelley, A. Banerjee, J. Yan, D. G. Mandrus, S. E. Nagler, and N. Ong, *Nat. Phys.* **17**, 915 (2021).
- [39] J. A. N. Bruin, R. R. Claus, Y. Matsumoto, N. Kurita, H. Tanaka, and H. Takagi, *Nat. Phys.* **18**, 401 (2022).
- [40] O. I. Motrunich, *Phys. Rev. B* **73**, 155115 (2006).
- [41] D. Chowdhury, I. Sodemann, and T. Senthil, *Nat. Commun.* **9**, 1 (2018).
- [42] I. Sodemann, D. Chowdhury, and T. Senthil, *Phys. Rev. B* **97**, 045152 (2018).